SCIENTIFIC REPORTS

OPEN

SUBJECT AREAS:
ATMOSPHERIC SCIENCES
PALAEOCLIMATE
PALAEONTOLOGY

Received
19 March 2014

Accepted
18 June 2014

Published
11 July 2014

Correspondence and requests for materials should be addressed to C.Q. (quan@jlu.edu.cn) or Y.-S.L. (liuc@etsu.edu)

Miocene shift of European atmospheric circulation from trade wind to westerlies

Cheng Quan[1], Yu-Sheng (Christopher) Liu[2], Hui Tang[3] & Torsten Utescher[4]

[1]Research Center of Paleontology and Stratigraphy, Jilin University, Changchun 130026, China, [2]Department of Biological Sciences, East Tennessee State University, Johnson City, Tennessee 37614, USA, [3]Department of Geosciences and Geography, University of Helsinki, Helsinki FI-00014, Finland, [4]Senckenberg Research Institute and Natural History Museum, Frankfurt Main; Steinmann Institute, Bonn University, Bonn 53115, Germany.

The modern European climatic regime is peculiar, due to its unitary winter but diverse summer climates and a pronounced Mediterranean climate in the south. However, little is known on its evolution in the deep time. Here we reconstruct the European summer climate conditions in the Tortonian (11.62–7.246 Ma) using plant fossil assemblages from 75 well-dated sites across Europe. Our results clearly show that the Tortonian Europe mainly had humid to subhumid summers and no arid climate has been conclusively detected, indicating that the summer-dry Mediterranean-type climate has not yet been established along most of the Mediterranean coast at least by the Tortonian. More importantly, the reconstructed distribution pattern of summer precipitation reveals that the Tortonian European must have largely been controlled by westerlies, resulting in higher precipitation in the west and the lower in the east. The Tortonian westerly wind field appears to differ principally from the trade wind pattern of the preceding Serravallian (13.82–11.62 Ma), recently deduced from herpetofaunal fossils. Such a shift in atmospheric circulation, if ever occurred, might result from the development of ice caps and glaciers in the polar region during the Late Miocene global cooling, the then reorganization of oceanic circulation, and/or the Himalayan-Tibetan uplift.

The Late Miocene, a critical time period in Cenozoic climatic evolution, saw profound environmental changes and geological events, which together regulated the then climate distribution pattern[1,2] and gradually propagated to modern climate configuration[3,4]. In North America a similar-to-modern climate was established as early as in the late Middle Miocene, marked by the onset of Great Plain landscape[5,6], while significantly intensified aridification in the vast Asian interior did not occur until the Late Miocene to Early Pliocene[3,6,7]. In Western Eurasia, however, although the Miocene climate has been extensively investigated[8–11], little is known about the early evolution of the regime, especially in regard to the hydrological dynamics and atmospheric circulation[6,11,12].

The modern Europe experiences a prevalence of westerlies in winter, while the summer climates are highly diverse, mainly consisting of a maritime climate along the western coast with evenly dispersed precipitation throughout the year, a Mediterranean climate in the south with dry summers, and a subhumid–semiarid continental climate to the east[13,14]. Such a pattern is jointly controlled by the westerlies and the seasonal shift of Azores subtropical high between ~30° N in winter and ~35° N in summer[4,14]. By contrast, during the Serravallian (late Middle Miocene; 13.82–11.62 Ma), the distribution of summer precipitation suggests that Europe was likely dominated by a trade wind system flowing from the northeast to southwest[15]. Therefore a dramatic shift of the wind field must have occurred between the Serravallian and present. However, neither proxy data nor modelling results have ever evidenced this upheaval before. Here we reconstruct the Tortonian (early Late Miocene; 11.62–7.246 Ma) hydrological dynamics of Europe using palaeobotanical proxy data supplemented by modelling experiments, with a specific focus on the summer condition, to infer the wind direction and consequently the prevailing atmospheric circulation patterns following the Serravallian. Our results reveal a dramatic transition in atmospheric circulation that the so called Serravallian trade winds[15] gave way to the Tortonian westerlies that predominate over Western Eurasia.

Results and Discussion

Tortonian summer hydrological distribution. The estimated means of warmest month precipitations (WMP) of the Tortonian Europe range between ~67 mm and ~164 mm, with corresponding warmest month temperatures (WMT) between 21.2°C and 27.8°C (Fig. 1A, 1B; and Supplementary Information Table 1 for complete data ranges). Locations with high WMPs are found in West Europe, except for the southerly coastal

regions of the Mediterranean, while relatively lower WMPs are mainly in the coastal areas of Lake Pannon and northern coast of the Black Sea to the east (Fig. 1A). In spite of the spatial differentiation of WMP and WMT, the overall summer climate of the Tortonian Europe was humid to subhumid, but with semi-arid to subhumid in the Andalucian coast of Spain, which is in agreement with the vegetation data, showing a latitudinal gradient[16,17] (Fig. 1C). No arid type is clearly detected according to the climatic

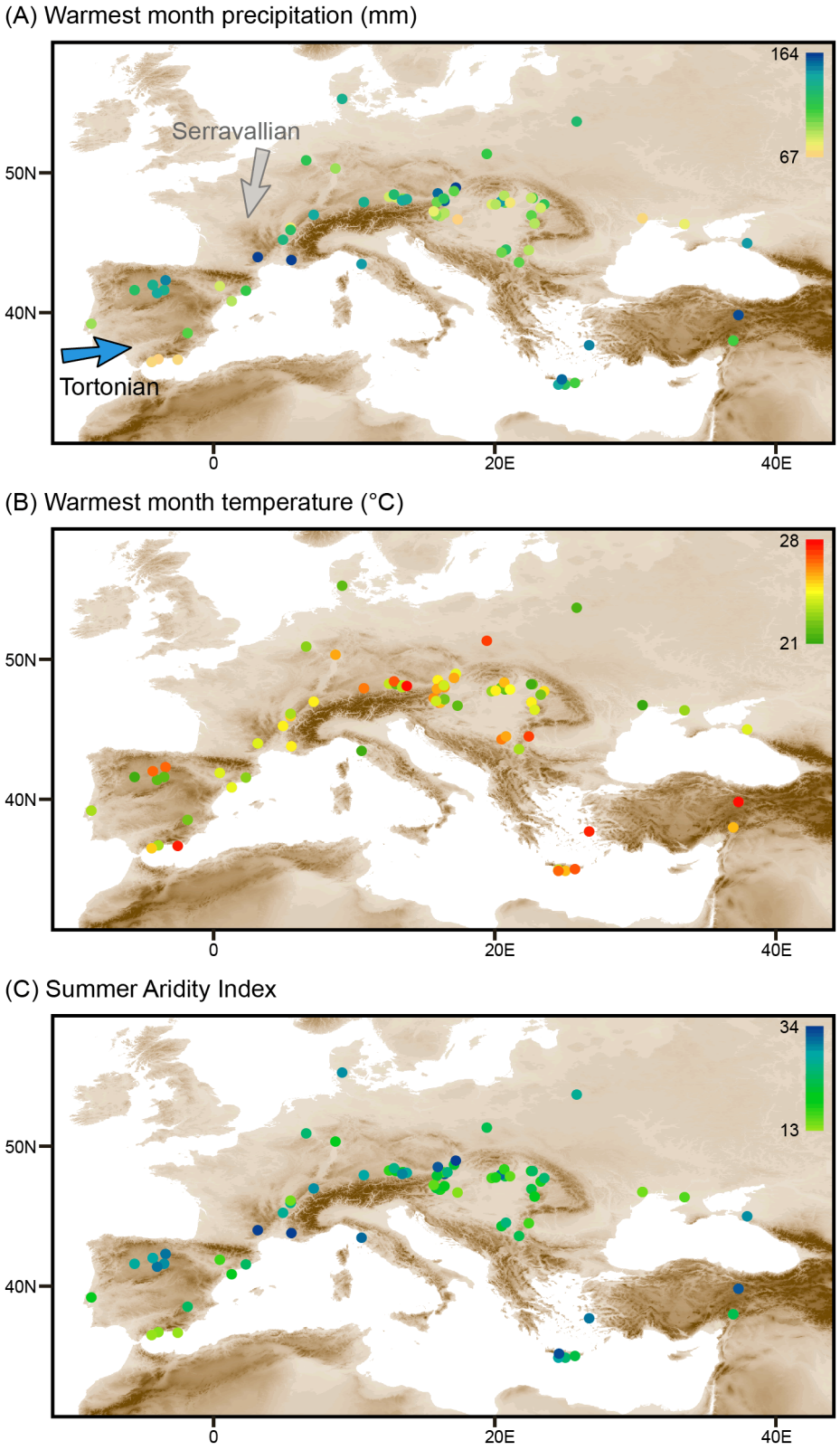

Figure 1 | Reconstruction of the Tortonian climate of Europe. (A) Warmest month precipitation. Arrows show direction of prevalent wind direction of particular age. The pink arrow denotes the Serravallian trade wind direction favored by European herpetofaunal data[15], while the blue arrow indicates the westerlies system inferred from the palaeobotanical data (this study). (B) Warmest month temperature. (C) Summer climatic condition described by Köppen Aridity Index. Palaeoclimatic data are available in Supplementary Information Table 1. The palaeoclimate maps were generated by ArcGIS, Esri.

classification of the Köppen Aridity Index (AI)[7] (Supplementary Information Table 1).

Humid to subhumid climates during the Tortonian throughout the major parts of Europe are also suggested by mammal hypsodonty data[6,18], small-mammal community structure[12], and herpetofaunal composition[19]. Although possibly punctuated by dry conditions in particular periods and/or at some locations, especially for that of the middle Tortonian northeastern Iberian Peninsula[20,21], both faunal and floral data indicate an overall (sub)humid climate in the Tortonian[3,4,6,12,18,22]. Moreover, it can be assumed that the Andalucian coastal area and the northern Black Sea coast experienced drier summers.

Notably our results show that humid to subhumid Tortonian summers existed in most of Europe, probably except for its southernmost parts (Fig. 1A). The spatial pattern of summer precipitation strongly indicates that the modern Mediterranean climate, with summer drought, had not yet been established by the Tortonian (Fig. 1C; Supplementary Information Table 1). This is in close agreement with fossil mammal community and the majority of palaeovegetation types from Spain, Italy, Greece, and Turkey, supporting the presence of evergreen broadleaved and mixed forests[12,23,24]. Although sclerophyll woodland and shrubland vegetation did occasionally occur in northeast Spain in the Late Miocene[3,4,16], it was likely resulted from a rain shadow effect caused by the uplift of metamorphic complexes at the basin margins[25]. Therefore, it appears that the northward migration of the subtropical high, which causes the modern Mediterranean dry summer must have had minimal impact on the Mediterranean summer during the Tortonian and affected only the southernmost parts.

Summer wind direction. Terrestrial rainfall in the extra-tropics is primarily controlled by wind transport of moisture from the oceans, with the total amount of precipitation decreasing towards continental interiors[11,14], while topography can cause local rain shadow effects[5,26]. Therefore, large-scale seasonal precipitation distribution can reflect well the associated wind direction given the moisture transport is the dominant factor in relation to precipitation[12,15]. The overall topography of Europe with huge mountains such as Alps and Pyrenees had largely been formed prior to the Late Miocene with exception of the final retreat of the Paratethys in the east[27–30].

Our quantitative palaeoclimate reconstruction suggests a zonal eastward decrease of summer precipitation in Tortonian Europe (Fig. 1A), as also implied by palaeovegetation types and mammal data[12,16]. This pattern clearly shows the dominant impact of westerlies on summer moisture transport and the existence of a high pressure system over the mid-latitudes of the Atlantic in summer that drove the moist air mass eastward from the ocean to the continent. However, the high pressure system must have been farther away from the European mainland than the modern Azores High, because the continental climate was mainly (sub)humid in the summer.

A rain shadow effect defined by local palaeotopography also indicates an overall westerly or south westerly wind in the Tortonian. For instance, WMPs experienced in the west of the Spanish Inner Plateau are much higher than those to the east (Fig. 1A). In addition, the WMPs to the south of the Alps are higher than those to the north, which indicates that the northward wind might also be important component of summer air flow in this region. In eastern Europe, the dominance of westerly wind can also be inferred by the relatively high WMPs in the coastal areas of Lake Pannon compared to that in the northern coast of Black Sea. Although the Tortonian WMP differentiations between two sides of plateaus or mountains are much less than those in the modern climate, the topographical effects in blocking water transport are evident (Fig. 1A).

Our inferences of the Tortonian summer wind direction based on WMPs are supported by the Tortonian climate model simulation. As illustrated in Fig. 2, there is relatively high pressure over north Atlantic and low pressure over central Eurasia in the warmest month in our Tortonian run (Fig. 2A), which leads to a strong westerly wind over Europe. Since the high pressure over the north Atlantic is more zonally oriented in the Tortonian run than that in the present-day run, the westerlies are intensified over most of Europe (Fig. 2B). This enhances advection of moisture and stormtracks[31], and hence precipitation over Europe in the Tortonian run. Additionally there is an increase of pressure over the Caspian and Black Sea regions in July in the Tortonian run (Fig. 2B). This may be due to the presence of the Paratethys and the cooler summer surface temperatures there. Such a high pressure anomaly might have contributed to the decrease of WMP particularly over the eastern Mediterranean in the Tortonian.

Both proxy and modeling results indicate that there was a subtropical high pressure system over the Atlantic (south) west to the European mainland in the Tortonian summers (Fig. 2), resulting in the Tortonian European mainland being dominated by westerlies, with an overall (sub)humid climate with the absence of Mediterranean climate type, probably except from its southernmost parts.

Possible shift of atmospheric circulation between Serravallian and Tortonian. The Tortonian wind direction deduced from the present study with a subtropical high in mid-latitudes around 40° N or so (Fig. 2A), is markedly different from conditions in the preceding Serravallian[15], suggesting a critical change in atmospheric circulation and hence climatic regime reorganization.

During the Serravallian summer, European fossil snakehead fish data exclusively suggest that a subtropical high pressure zone situated over northeast to east Europe around 47°N[15] drove winds (south)-westward over Europe[15,32]. If this hypothesis is further confirmed, then the Serravallian–Totonian transition must have seen a nearly orthogonal shift of the atmospheric circulation over Europe, associated with a southwestern shift of the subtropical high (Fig. 1A).

The southwestward subtropical high shift might be the result of ephemeral Tortonian glaciation after the broadly ice-free Serravallian in the northern hemisphere oceans. Biostratigraphical and isotopic records from northernmost Atlantic undoubtedly indicate a major cooling event in the earliest Tortonian (~11 Ma)[33], and furthermore coarse-fraction compositions in ocean sediments show a clear signal of nearly coeval seasonal sea-ice cover in the region between Greenland and Svalbard associated with a cold East Greenland current[34]. On the one hand, the early accumulation of ice caps and glaciers in north polar regions in the Tortonian[2] must considerably have, although not totally, offset the hemispherical asymmetry of atmospheric circulation by oceanic currents[1] and forced the high pressure system to cooler region in the summer. On the other hand, marine microfossils strongly suggest that the Fram Strait between Greenland and Svalbard was considerably deepened at ~11 Ma[35], which together with the East Greenland current may have jointly resulted in a fundamental reorganization of oceanic circulation[36], contributing to the palaeo-North Atlantic gyre[37] and palaeo-Azores High[19]. In addition, the remarkable development of Himalayan–Tibetan system in both elevation and extension[38] would have enhanced the reign of low pressure over Eurasian land mass in summer by increasing land–sea heat capacity differentiation[39], which strikingly reinforced a longitudinally pressure gradient[40] and modified global atmospheric circulation[26].

The Tortonian subtropical high over the Atlantic deviated southward or southeastward during the late Messinian as evidenced by the significant aridification in the Iberian Peninsula[6,12,18,21] and the Mediterranean Messinian Salinity Crisis[41]. However, it appears that the Mediterranean climate type may have not been established until the subtropical high arrived at its near-modern position in the Late Pliocene to Pleistocene[4] when ice-sheets were fully developed in both hemispheres[2], which finally resulted in the modern atmospheric circulation and climatic distribution pattern[42].

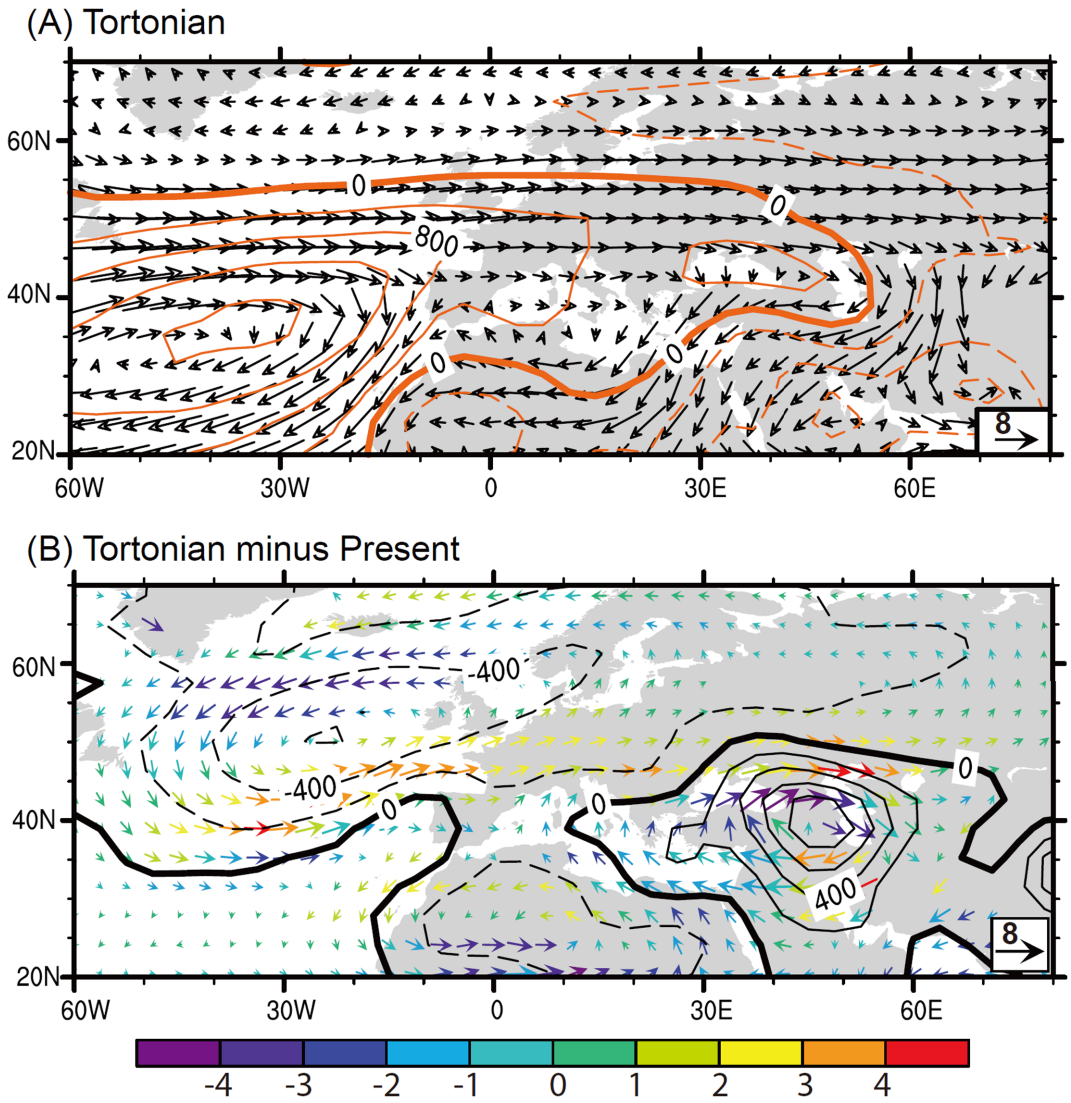

Figure 2 | (A) 850 hPa wind (vector; m/s) and sea level pressure anomalies (Pa) to global average (contour) in July in the Tortonian global simulation[31]. (B) Difference of 850 hPa wind (vector; m/s) and sea level pressure (Pa) in July between the Tortonian and present-day global simulation. The coloured vectors denoted the changes in wind speed (m/s), which are significant with a Student's *t*-test ($p < 0.05$). Maps were created by the NCAR Command Language.

It is noted that so far, climate model simulations for the Middle Miocene and Late Miocene have not demonstrated any significant transition of atmospheric circulation over Europe between these two time intervals[31,43–45]. In particular, climate models do not show a pronounced northward shift of the Inter-Tropical Convergence Zone (ITCZ) and the subtropical high pressure zone in the Middle Miocene as suggested by proxy data[15]. Such discrepancy could be either due to the misinterpretation of these proxy records, or possibly to the failure of the climate models to represent the natural climate variability in deep time. It is widely known that current climate models tend to underestimate temperature increase over high latitudes in the warm geological intervals including the Middle Miocene[31,43,46,47]. This can lead to an underestimation of the northward shift of ITCZ and the subtropical high in these stages. In addition, it is still highly uncertain how the presence of Paratethys and Tethys seaways had affected the ocean and atmospheric circulation over Europe in the Middle–Late Miocene[48], which would be highly interesting to study this phenomenon using fully coupled climate models in the future.

Conclusions

Deep time atmospheric circulation is one of the hardest palaeoenvironmental factors to be estimated due to the deficiency in records of wind direction. Because of the close relationship between atmospheric circulation and precipitation distribution at the continental scale, this dilemma can now be tackled. In the present study, fossil plant based climate reconstructions show that the Tortonian Europe had mostly humid to subhumid insummers. On the one hand, the absence of (semi-)arid conditions in the Central Mediterranean indicates that a Mediterranean-type climate had not yet established at least until the Tortonian. On the other hand, the spatial pattern of precipitation implies that the Tortonian Europe must have been under the dominance of westerlies in summer, with a higher precipitation in most of the western continent and relatively lower in the eastern parts. The prevalence of Tortonian westerlies field further implies a dramatic shift of the wind field and consequently a critical transition of atmospheric circulation from that in the preceding Serravallian. Such a shift in wind field over the European mainland might be a response to the Late Miocene global cooling. However, further study is needed to reveal pre- and post-Tortonian development of the Azores subtropical high, which is essential for the modern climatic configuration of Europe.

Methods

Palaeoclimate reconstruction. Proxy-based climate data are obtained from a total of 75 European palaeofloras comprising pollen and spores, leaf floras, and carpological

records. All floras are dated as Tortonian, based on various sources of evidence (Supplementary Information Table 1)[11,49,50]. Some of the investigated floras were already published in the frame of research conducted by the NECLIME network and are available in the PANGAEA database (www.pangaea.de)[11], while others are analyzed by this study (Supplementary Information Table 1). Climate data for some of the sites may slightly differ with respect to the published values due to revised taxonomy and/or updates in the concept of nearest living relatives (NLRs) of fossil taxa and their climatic requirements. The complete data set used in this study is provided in the supplementary materials. All floras were analyzed using the Coexistence Approach (CA)[51]. The method is based on the assumption that the climatic requirements of fossil plant taxa are similar to those of their NLRs. With the CA, for each climate parameter the climatic ranges in which a maximum number of NLRs of a given fossil flora can coexist is determined independently and considered the best description of the palaeoclimatic situation under which the given fossil flora lived. In this study, mean warmest month temperature (WMT) and warmest month precipitation (WMP) are considered as variables. The resolution of the CA strongly depends on the number of NLRs contributing with climate data in the analysis (10 to 74 in the present study). Hence, lower diversity of some of the floras may lead to rather broad ranges of climate variables (Supplementary Information Table 1), a data quality to be considered when interpreting spatial patterns.

The palaeohydrological condition of the climatic type is defined by Köppen Aridity Index (AI)[7]. The AI is calculated by annual precipitation divided by mean annual temperature plus a constant, based on which the humidity/aridity conditions can be classified into 5 categories (humid, subhumid, semi-arid, arid, and hyper-arid, respectively)[7]. To understand the summer palaeohydrological condition in the concept of AI category, we use the following formula to calculate warmest month AI that defines the summer hydrological condition:

$$AI = \frac{\mathrm{WMP} \times 12}{\frac{\mathrm{WMT} \times 12}{12} + 33} \quad (1)$$

The means of CA intervals were used in the calculation, because they are considered as appropriate in visualising climatic trends between regions, especially when interpolating over greater distances[11]. We further infer the summer wind direction based on the overall distribution of WMP, based on the assumption that the large-scale pattern of continental precipitation is mainly affected by the wind that transporting moisture[14].

Tortonian climate model simulation. To better demonstrate the atmospheric circulation changes implied by our WMP reconstruction, a Tortonian climate modelling study based on a fully coupled global climate model (ECHAM5/MPI-OM)[31] was employed. The resolution of the atmosphere general circulation model ECHAM5 is T31 ($3.75^\circ \times 3.75^\circ$) with 19 terrain-following vertical layers. The ocean circulation model MPIOM has an approximate resolution of $3^\circ \times 3^\circ$ and the vertical domain is represented by 40 unevenly spaced levels. To better represent the climate in the Tortonian, the physical boundary conditions in the model were modified[31]. For instance, the orography is generally reduced. In particular, Greenland was much lower than today because of the removal of the modern ice sheet, and the Alps and the Tibetan Plateau are generally reduced to 70% of present- day height. The land–sea distribution in the Tortonian model setup is largely the same as today, except for the presence of the Paratethys Sea and the Pannon Lake. There is also an open Indonesian Seaway and an open Panama Isthmus with a depth of 500 m in the ocean model. The Tortonian vegetation is characterized by a larger-than-present forest cover and less desert. Particularly, the present-day deserts in central Asia and Sahara are replaced by grassland and savanna. The boreal forests extend far more into the high latitudes including Greenland. The CO_2 concentration in the Tortonian simulation is set to 360 ppm which lies in the range of the estimated CO_2 concentration for the Late Miocene (200–400 ppm) based on different proxy data. The orbital parameters were chosen the same as present-day. More details on the model specifications and model performance are described in ref. 31.

1. Rea, D. K. The paleoclimatic record provided by eolian deposition in the deep sea: The geologic history of wind. *Rev. Geophys.* **32**, 159–195 (1994).
2. Zachos, J., Pagani, M., Sloan, L., Thomas, E. & Billups, K. Trends, rhythms, and aberrations in global climate 65 Ma to present. *Science* **292**, 686–693 (2001).
3. Pound, M. J., Haywood, A. M., Salzmann, U. & Riding, J. B. Global vegetation dynamics and latitudinal temperature gradients during the Mid to Late Miocene (15.97–5.33 Ma). *Earth Sci. Rev.* **112**, 1–22 (2012).
4. Suc, J. P. Origin and evolution of the Mediterranean vegetation and climate in Europe. *Nature* **307**, 429–432 (1984).
5. Mulch, A., Sarna–Wojcicki, A. M., Perkins, M. E. & Chamberlain, C. P. A Miocene to Pleistocene climate and elevation record of the Sierra Nevada (California). *Proc. Natl Acad. Sci.* **105**, 6819–6824 (2008).
6. Eronen, J. T. *et al*. Neogene aridification of the Northern Hemisphere. *Geology* **40**, 823–826 (2012).
7. Quan, C., Han, S., Utescher, T., Zhang, C. & Liu, Y. S. C. Validation of temperature–precipitation based aridity index: Paleoclimatic implications. *Palaeogeogr. Palaeoclimatol. Palaeoecol.* **386**, 86–95 (2013).
8. Popova, S., Utescher, T., Gromyko, D., Bruch, A. A. & Mosbrugger, V. Palaeoclimate evolution in Siberia and the Russian Far East from the Oligocene to Pliocene: Evidence from fruit and seed floras. *Turkish J. Earth Sci.* **21**, 315–334 (2012).
9. Popova, S. *et al*. Vegetation change in Siberia and the northeast of Russia during the Cenozoic cooling: A study based on diversity of plant functional types. *PALAIOS* **28**, 418–432 (2013).
10. Utescher, T., Djordjevic–Milutinovic, D., Bruch, A. & Mosbrugger, V. Palaeoclimate and vegetation change in Serbia during the last 30 Ma. *Palaeogeography, Palaeoclimatology, Palaeoecology* **253**, 141–152 (2007).
11. Bruch, A. A., Utescher, T. & Mosbrugger, V. Precipitation patterns in the Miocene of Central Europe and the development of continentality. *Palaeogeogr. Palaeoclimatol. Palaeoecol.* **304**, 202–211 (2011).
12. van Dam, J. A. Geographic and temporal patterns in the late Neogene (12–3 Ma) aridification of Europe: The use of small mammals as paleoprecipitation proxies. *Palaeogeogr. Palaeoclimatol. Palaeoecol.* **238**, 190–218 (2006).
13. Vines, R. G. European rainfall patterns. *J. Climatol.* **5**, 607–616 (1985).
14. Rohli, R. V. & Vega, A. J. *Climatology* (Jones and Bartlett Publishers, 2008).
15. Böhme, M. Migration history of air-breathing fishes reveals Neogene atmospheric circulation patterns. *Geology* **32**, 393–396 (2004).
16. Jiménez–Moreno, G., Fauquette, S. & Suc, J. P. Miocene to Pliocene vegetation reconstruction and climate estimates in the Iberian Peninsula from pollen data. *Rev. Palaeobot. Palynol.* **162**, 403–415 (2010).
17. Jiménez-Moreno, G. *Utilización del análisis polínico para la reconstrucción de la vegetación, clima y estimación de paleoaltitudes a lo largo de arco alpino europeo durante el Mioceno (21-8 Ma)* Ph.D. thesis, Universidad de Granada, (2005).
18. Fortelius, M. *et al*. Fossil mammals resolve regional patterns of Eurasian climate change over 20 million years. *Evol. Ecol. Res.* **4**, 1005–1016 (2002).
19. Böhme, M., Ilg, A. & Winklhofer, M. Late Miocene "washhouse" climate in Europe. *Earth Planet. Sci. Lett.* **275**, 393–401 (2008).
20. Böhme, M., Winklhofer, M. & Ilg, A. Miocene precipitation in Europe: Temporal trends and spatial gradients. *Palaeogeogr. Palaeoclimatol. Palaeoecol.* **304**, 212–218 (2011).
21. Domingo, L. *et al*. Late Neogene and Early Quaternary Paleoenvironmental and Paleoclimatic Conditions in Southwestern Europe: Isotopic Analyses on Mammalian Taxa. *PLoS ONE* **8**, e63739 (2013).
22. van Dam, J. A. & Weltje, G. J. Reconstruction of the Late Miocene climate of Spain using rodent palaeocommunity successions: An application of end–member modelling. *Palaeogeogr. Palaeoclimatol. Palaeoecol.* **151**, 267–305 (1999).
23. Utescher, T., Erdei, B., François, L. & Mosbrugger, V. Tree diversity in the Miocene forests of Western Eurasia. *Palaeogeogr. Palaeoclimatol. Palaeoecol.* **253**, 226–250 (2007).
24. Pound, M. J. *et al*. A Tortonian (Late Miocene, 11.61–7.25 Ma) global vegetation reconstruction. *Palaeogeogr. Palaeoclimatol. Palaeoecol.* **300**, 29–45 (2011).
25. Krijgsman, W. *et al*. The 'Tortonian salinity crisis' of the eastern Betics (Spain). *Earth Planet. Sci. Lett.* **181**, 497–511 (2000).
26. Molnar, P., Boos, W. R. & Battisti, D. S. Orographic controls on climate and paleoclimate of Asia: Thermal and mechanical roles for the Tibetan Plateau. *Ann. Rev. Earth Planet. Sci.* **38**, 77–102 (2010).
27. Sinclair, H. D., Gibson, M., Naylor, M. & Morris, R. G. Asymmetric growth of the Pyrenees revealed through measurement and modeling of orogenic fluxes. *Ame. J. Sci.* **305**, 369–406 (2005).
28. Popov, S. V. *et al*. Late Miocene to Pliocene palaeogeography of the Paratethys and its relation to the Mediterranean. *Palaeogeogr. Palaeoclimatol. Palaeoecol.* **238**, 91–106 (2006).
29. Campani, M., Mulch, A., Kempf, O., Schlunegger, F. & Mancktelow, N. Miocene paleotopography of the Central Alps. *Earth Planet. Sci. Lett.* **337–338**, 174–185 (2012).
30. Jiménez–Moreno, G., Fauquette, S. & Suc, J. P. Vegetation, climate and palaeoaltitude reconstructions of the Eastern Alps during the Miocene based on pollen records from Austria, Central Europe. *J. Biogeogr.* **35**, 1638–1649 (2008).
31. Micheels, A. *et al*. Analysis of heat transport mechanisms from a Late Miocene model experiment with a fully–coupled atmosphere–ocean general circulation model. *Palaeogeogr. Palaeoclimatol. Palaeoecol.* **304**, 337–350 (2011).
32. Unger, H. J., Fiest, W. & Niemeyer, A. Die Bentonite der Ostbayerischen Molasse und ihre Beziehungen zu den Vulkaniten des Pannonischen Beckens. *Geol. Jahrb.* **96, ser. D**, 67–112 (1990).
33. Fronval, T. & Jansen, E. Late Neogene paleoclimates and paleoceanography in the Iceland–Norwegian Sea: Evidence from the Iceland and Vøring Plateaus. *Proc. Ocean Drill. Program Sci. Results* **151**, 455–468 (1996).
34. Wolf–Welling, T. C. W., Cremer, M., O'Connell, S., Winkler, A. & Thiede, J. Cenozoic Arctic gateway paleoclimate variability: Indications from changes in coarse–fraction composition. *Proc. Ocean Drill. Program Sci. Results* **151**, 515–567 (1996).
35. Matthiessen, J., Brinkhuis, H., Poulsen, N. & Smelror, M. Decahedrella martinheadii Manum 1997–A stratigraphically and paleoenvironmentally useful Miocene acritarch of the high northern latitudes. *Micropaleontology* **55**, 171–186 (2009).
36. Schreck, M., Matthiessen, J. & Head, M. J. A magnetostratigraphic calibration of Middle Miocene through Pliocene dinoflagellate cyst and acritarch events in the Iceland Sea (Ocean Drilling Program Hole 907A). *Rev. Palaeobot. Palynol.* **187**, 66–94 (2012).
37. Benson, R. H., Rakic–El Bied, K. & Bonaduce, G. An important current reversal (influx) in the Rifian Corridor (Morocco) at the Tortonian–Messinian boundary: The end of Tethys Ocean. *Paleoceanography* **6**, 165–192 (1991).

38. Harrison, T. M., Copeland, P., Kidd, W. S. F. & Yin, A. Raising Tibet. *Science* **255**, 1663–1670 (1992).
39. Zhisheng, A., Kutzbach, J. E., Prell, W. L. & Porter, S. C. Evolution of Asian monsoons and phased uplift of the Himalaya–Tibetan plateau since Late Miocene times. *Nature* **411**, 62–66 (2001).
40. Rea, D. K. & Bloomstine, M. K. Neogene history of the south Pacific tradewinds: Evidence for hemispherical asymmetry of atmospheric circulation. *Palaeogeogr. Palaeoclimatol. Palaeoecol.* **55**, 55–64 (1986).
41. Clauzon, G., Suc, J. P., Gautier, F., Berger, A. & Loutre, M. F. Alternate interpretation of the Messinian salinity crisis: Controversy resolved? *Geology* **24**, 363–366 (1996).
42. Sadori, L. *et al.* Palynology and Mediterranean vegetation history. *Flora Mediterranea* **23**, 141–156 (2013).
43. Herold, N., Huber, M. & Müller, R. D. Modeling the Miocene Climatic Optimum. Part I: Land and Atmosphere. *J. Clim.* **24**, 6353–6372 (2011).
44. Henrot, A. J. *et al.* Effects of CO_2, continental distribution, topography and vegetation changes on the climate at the Middle Miocene: a model study. *Clim. Past* **6**, 675–694 (2010).
45. Steppuhn, A., Micheels, A., Geiger, G. & Mosbrugger, V. Reconstructing the Late Miocene climate and oceanic heat flux using the AGCM ECHAM4 coupled to a mixed–layer ocean model with adjusted flux correction. *Palaeogeogr. Palaeoclimatol. Palaeoecol.* **238**, 399–423 (2006).
46. Micheels, A., Bruch, A. A., Uhl, D., Utescher, T. & Mosbrugger, V. A Late Miocene climate model simulation with ECHAM4/ML and its quantitative validation with terrestrial proxy data. *Palaeogeogr. Palaeoclimatol. Palaeoecol.* **253**, 251–270 (2007).
47. You, Y., Huber, M., Müller, R. D., Poulsen, C. J. & Ribbe, J. Simulation of the Middle Miocene Climate Optimum. *Geophys. Res. Lett.* **36**, L04702 (2009).
48. Hamon, N., Sepulchre, P., Lefebvre, V. & Ramstein, G. The role of eastern Tethys seaway closure in the Middle Miocene Climatic Transition (ca. 14 Ma). *Clim. Past* **9**, 2687–2702 (2013).
49. Utescher, T., Böhme, M. & Mosbrugger, V. The Neogene of Eurasia: Spatial gradients and temporal trends – The second synthesis of NECLIME. *Palaeogeogr. Palaeoclimatol. Palaeoecol.* **304**, 196–201 (2011).
50. Bruch, A. A., Uhl, D. & Mosbrugger, V. Miocene Climate in Europe – patterns and evolution. First synthesis of NECLIME. *Palaeogeogr. Palaeoclimatol. Palaeoecol.* **253**, 1–7 (2007).
51. Mosbrugger, V. & Utescher, T. The coexistence approach–A method for quantitative reconstructions of Tertiary terrestrial palaeoclimate data using plant fossils. *Palaeogeogr. Palaeoclimatol. Palaeoecol.* **134**, 61–86 (1997).

Acknowledgments

We thank Profs. Bob Spicer, Jean-Pierre Suc, and Gaojun Li for their thoughtful comments and suggestions, Dr. Arne Micheels for providing the model results, Dr. Jussi Eronen for helpful comments, Drs. E. Favre, G. Jiménez-Moreno, and A. Bruch for providing helpful floral data, and Edward Liu for reading the manuscript. Funds for this research were provided by NBRP 2012CB822003, NSFC 41172008 and 41372002, U.S. NSF EAR–0746105, DFG 455, and BiK F and DFG MI 926/8–1.

Author contributions

C.Q., Y.S.L. and T.U. conceived and designed research. C.Q., Y.S.L. and H.T. performed research; C.Q., Y.S.L., H.T. and T.U. analyzed and interpreted data; C.Q. and Y.S.L. wrote the paper.

Additional information

Supplementary information accompanies this paper at http://www.nature.com/scientificreports

Competing financial interests: The authors declare no competing financial interests.

How to cite this article: Quan, C., (Christopher) Liu, Y.-S., Tang, H. & Utescher, T. Miocene shift of European atmospheric circulation from trade wind to westerlies. *Sci. Rep.* **4**, 5660; DOI:10.1038/srep05660 (2014).